

Methods for isolating coherent noise in the Radon domain

Shauna K. Oppert and R. James Brown

ABSTRACT

Discrete Radon transforms are often employed for the discrimination of reflections having parabolic or hyperbolic moveout, with no variation in amplitude with offset. The present work has tested the effects of data weighting and variants of the Radon transform for primary, multiple, and mode-converted reflections on a flat-lying model. Data weighting prior to the application of a Radon transform allowed for accurate identification of mode-converted reflections from other events. The pre- and postcritical energy from the mode-converted reflection was successfully separated in the Radon domain through application of a multiple-hyperbolic and a fourth-order nonhyperbolic Radon transform on separate near- and far-offset panels. Focusing of events in the Radon domain was maximized when we used a t^2 -stretched parabolic transform or a fourth-order nonhyperbolic transform tuned for mode-converted reflections. Additional work is necessary to improve the robustness of the algorithms.

INTRODUCTION

The discrete Radon transform integrates data along curved surfaces in the time-offset (t - x) domain in order to transform parabolic or hyperbolic events into points in the Radon domain. The Radon transform is typically employed in the suppression of random noise, interpolation for missing traces, and removal of coherent events (e.g. ground roll and multiples). After implementation of a Radon transform, a better estimate of stacking velocities can often be obtained. Unfortunately, muting in the Radon domain can alter near-offset amplitudes in primary events, effecting AVO analysis (Kabir and Marfurt, 1999). Smearing and defocusing of events in the Radon domain can be due to assuming events maintain a parabolic or hyperbolic shape. Furthermore, the nonuniqueness of the inverse transforms leads to discrepancies in the transformed and original data sets.

Thorson and Claerbout (1985) describe some implicit assumptions made in using the Radon transform on regular data. A reflector on a CMP gather should have uniform amplitude and vary smoothly in moveout from trace to trace for the Radon transform to be able to effectively focus the event. Specifically, the traces on the gather must be free of static shifts and be balanced in amplitude. In order to avoid problems due to violating these assumptions, the data should be preconditioned prior to Radon analysis to remove dip, static problems, and even amplitude variations with offset. Part of this work aims to provide a data preconditioning method for discriminating coherent events based on amplitude variations in offset. The method proposed involves offset weighting of the data prior to application of the Radon transform. In addition, separate Radon transforms are applied to the near and far offsets independently to compare effects of a phase change at the critical angle.

Four Radon transform variants are used to isolate reflections, including: the parabolic, the t^2 -stretched parabolic, the multiple-hyperbolic, and the fourth-order nonhyperbolic transforms. The transforms were applied in a discrete Radon

algorithm. It is important to note that better focusing and resolution is expected from a generalized high-resolution algorithm, such as that proposed by Sacchi and Ulrych (1995), and future work will employ such a method.

The model used in data analysis includes a base-of-salt primary reflection, a salt-bed multiple, and a salt-bed PSSP mode-converted reflection. In typical marine surveys over salt, long offsets are required for imaging subsalt reflectors. Using a typical hyperbolic transform for summation of reflectors may involve an inadequate approximation for nonhyperbolic long-offset data, causing amplitude smearing in the Radon domain. Taner and Koehler (1969) and Castle (1994) described a recursive equation for n th-order approximations of the NMO equation. Carlson (1997) employed the fourth-order equation for NMO correction of long-offset data. In this work, the fourth-order NMO equation for the Radon transformation is utilized for focusing of nonhyperbolic, long-offset data.

METHODS

Discrete Radon transform

The formulation of the discrete Radon transform used in this work follows the least-squares technique described by Foster and Mosher (1992). The Radon transform, ϕ , is given as:

$$\phi(p, \tau) = \int_{x_{\min}}^{x_{\max}} \psi(x, \underline{t}) dx, \quad (1)$$

where $\psi(x, t')$ represents the data in the time domain, p is slowness, τ is the zero-offset traveltime, and x is offset. The traveltime \underline{t} represents the summation curves of the input data. The input time vector is t for typical parabolic curves and t^2 for stretched parabolic and fourth-order nonhyperbolic curves. Slant stacks sum energy along lines represented by: $t = \tau + px$, while parabolic transforms sum along curves of $t = \tau + px^2$. The t^2 -stretched parabolic transform uses a traveltime input of $\underline{t} = t^2$, which makes hyperbolic reflections in the x - t domain approximately parabolic in the x - t^2 domain. The stretched transform sums along $t^2 = \tau^2 + p^2 x^2$ parabolic curves in the x - t^2 domain (Yilmaz, 1989). Foster and Mosher (1992) presented a traveltime curve for summing hyperbolic multiple reflections where $t = \tau + p \left(\sqrt{(x_k)^2 + z^2} - z \right)$ is the path of summation, and z is a chosen depth to focus the multiple reflection. The fourth-order nonhyperbolic transform employs a fourth-order NMO function for the summation of reflections and is explained later in more detail.

The integration of curved lines in the time domain is similar to the integration of phase shifts in the Fourier domain. A forward Fourier transform is applied to the data to facilitate integration. The transformed data is written as:

$$\tilde{\phi}(p, \omega) = \int_{x_{\min}}^{x_{\max}} \tilde{\psi}(x, \omega) e^{i\omega(\underline{t}(x,p) - \tau)} dx. \quad (2)$$

When working with discrete data, it is easier to express (2) as a summation:

$$\tilde{\phi}(p_j, \omega) = \sum_{k=1}^N \tilde{\psi}(x_k, \omega) e^{i\omega(\underline{t}(x_k, p_j) - \tau)} \Delta x_k, \{1, \dots, N\}. \quad (3)$$

Concisely put, the summation can be written in matrix form as:

$$\phi_\omega(p_j) = \underline{R} z_\omega(\underline{t}(x_k)), \quad (4)$$

where \underline{R} is an $M \times N$ matrix with elements:

$$R_{jk} = e^{i\omega(\underline{t}(x_k, p_j) - \tau)} \Delta x_k, \{j = 1, \dots, M; k = 1, \dots, N\}. \quad (5)$$

The Hermitian conjugate of \underline{R} , \underline{R}^H , allows for a least-squares formula of ϕ , where

$$\phi_\omega(p_j) = [\underline{R} \underline{R}^H] \underline{R} z_\omega(\underline{t}(x_k)) \quad (6)$$

(Foster and Mosher, 1992). This method is solved independently for each frequency, and as a result, some smearing of amplitudes in the Fourier domain occurs.

Fourth-order NMO equation

Taner and Koehler (1969) give the following equation for traveltimes:

$$t^2 = c_1 + c_2 x^2 + c_3 x^4 + \dots, \quad (7)$$

where

$$c_1 = t_0^2, \quad (8)$$

$$c_2 = \frac{1}{\mu_2}, \quad (9)$$

$$c_3 = \frac{1}{4} \frac{\mu_2^2 - \mu_4}{t_0^2 \mu_2^4}, \quad (10)$$

and

$$\mu_j = \frac{\sum_{k=1}^N \Delta \tau_k V_k^j}{\sum_{k=1}^N \Delta \tau_k}. \quad (11)$$

In this work, we use the three-term expression in equation (7) for summation curves in the fourth-order hyperbolic Radon transform. The t_0 and μ_4 focusing parameters for a particular primary, multiple, or converted-wave reflection are extrapolated from the data set as input parameters.

DATA ANALYSIS

One flat-layered 2-D model was used for Radon comparison and the parameters for the model are given in Table 1. The seismogram (Figure 1a) was generated using Norsar-2D modeling software, and automatic gain control (AGC) was applied using ProMAX[®] software. The Radon transforms were performed and analyzed using Matlab programs. The amplitude scale for each Radon-domain plot is labeled to the right of each diagram.

Table 1: Parameters for model

Layer	P Velocity (m/s)	S Velocity (m/s)	Thickness (m)
1	1500		1000
2	2040		800
3	2160		800
4	4500	2600	1000

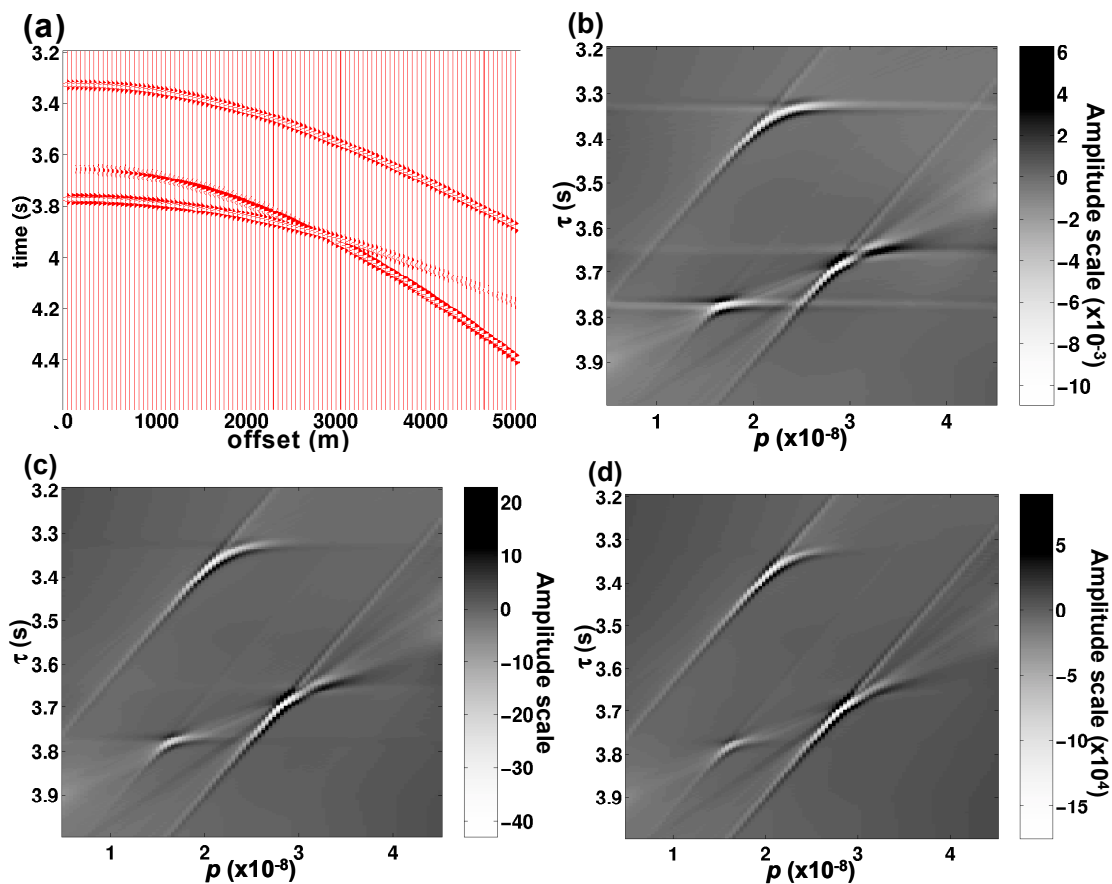


FIG. 1. (a) The CMP gather for the base-of-salt P-reflection ($t_0=3.3s$), the salt-bed PSSP reflection ($t_0=3.63s$), and salt-bed multiple ($t_0=3.75s$) used in the analysis. (b) The parabolic Radon transform for the data. (c) and (d) The offset-weighted and offset-squared-weighted parabolic Radon transforms of the data, respectively.

The application of the parabolic Radon transform to the unweighted data is shown in Figure 1b. Each event is distinctly separated, although limited aperture of far offsets causes increased smearing of energy diagonally from the bottom left to the top

right of the diagram (Figure 1b) (while near-offset horizontal smearing is reduced). A far-offset taper may be applied to the data prior to the transform to reduce the diagonal smearing caused by limited aperture (Kabir and Marfurt, 1999). The parabolic transforms of the offset-weighted and offset-squared-weighted data are depicted in Figures 1c and d. By placing more importance on far offsets with weighting, multiple energy is suppressed while the converted energy is enhanced. Unlike multiple or primary events, PSSP mode-converted energy increases in amplitude with offset. The diagrams indicate that offset weighting can provide a discriminator for detecting converted energy from primary and especially multiple events on a CMP gather. The actual focusing power of data weighting is difficult to determine due to the low resolution of the least-squares transform.

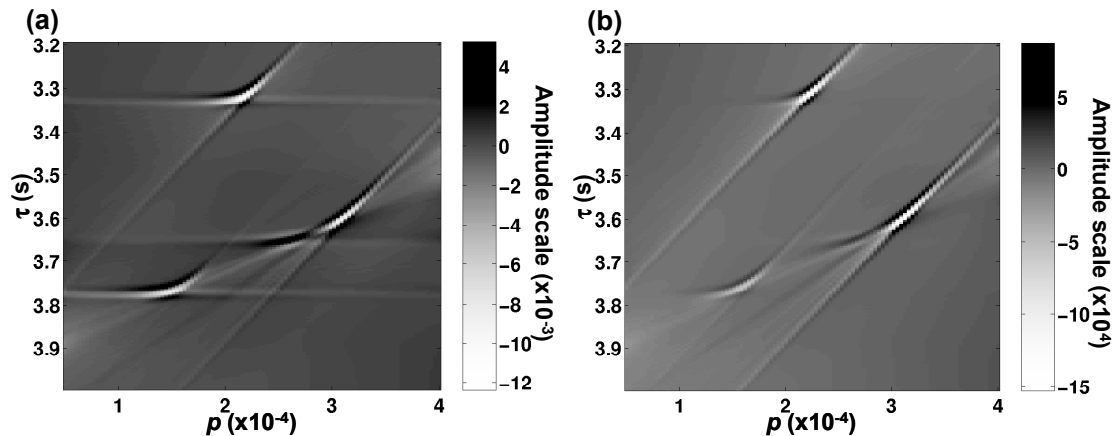


FIG. 2. (a) The hyperbolic multiple Radon transform was applied to the original data set and (b) to the offset-squared weighted data.

Foster and Mosher's (1992) hyperbolic Radon transform for multiples was applied to the data and offset-squared data in Figures 2a and b. The transform creates 'smiles' at the focusing points for reflections, indicating an inaccurate approximation and overcorrection of events. A significant quality of the transform is its ability to separate near-offset energy from that of far offsets for the converted-wave reflection in Figure 2a. Although smearing is a factor, the near-offset energy is focused on the slowness axis at about 0.00026 s/m and the far-offset energy focuses around 0.00030 s/m.

The fourth-order hyperbolic equation was used in the transform of data in Figures 3a, b, and c. The t_0 and μ_4 focusing parameters for the reflectors were estimated from the data. The focusing parameters for the primary event focused the primary and multiple events, while leaving the energy from the converted-wave diminished in the Radon domain (Figure 3a). Good focusing and reduced smearing was observed for all events when using the parameters for the converted-wave event (Figure 3b).

The parameters for the multiple event caused smearing of all events except for the multiple energy (Figure 3c). Figures 3a, b, and c (fourth-order hyperbolic) can be compared to Figure 3d (t^2 -stretched parabolic). The data stretching improved focusing of all events, in comparison with the result of the parabolic transform on unstretched data (Figure 1b). The focusing of events by the fourth-order hyperbolic transform

tuned for the converted-wave reflection (Figure 3b) appears to be comparable to that of the t^2 -stretched parabolic transformed data (Figure 3d).

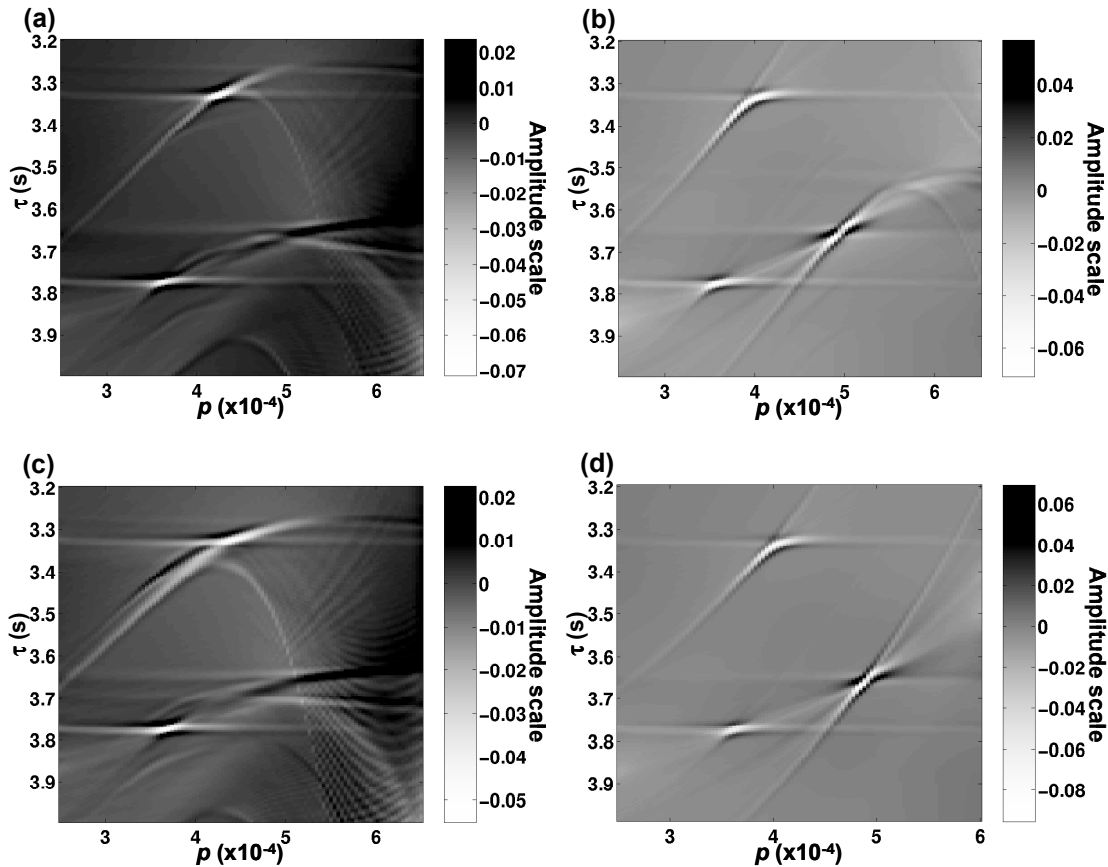


FIG. 3. The fourth-order hyperbolic Radon transform was applied to the data. The parameters t_0 and μ_4 were estimated from the data: (a) for the primary reflection, (b) for the converted wave, and (c) for the multiple event. (d) The t^2 -stretched parabolic Radon transform was applied to the data.

Figure 4 shows the result of applying the fourth-order hyperbolic Radon transform to near and far offsets separately. The data were separated at the 90° phase change at the critical angle for the converted-wave event. As a result, the focused converted-wave energy is of opposite polarity for each group of offsets. The primary and multiple energies are well focused in each panel, and do not show a similar phase change. The diagrams indicate this process has successfully separated energies from each phase rotation in the converted-wave reflection.

DISCUSSION

Kabir and Marfurt (1999) show that tapering near offsets prior to transformation increases smearing in the Radon domain, while tapering far offsets has the opposite effect. Contrary to what might be expected, applying offset weighting does not increase smearing on the near offset data, as indicated by a lack of horizontal smearing on the focusing events in the Radon domain (Figures 1c and 1d). The

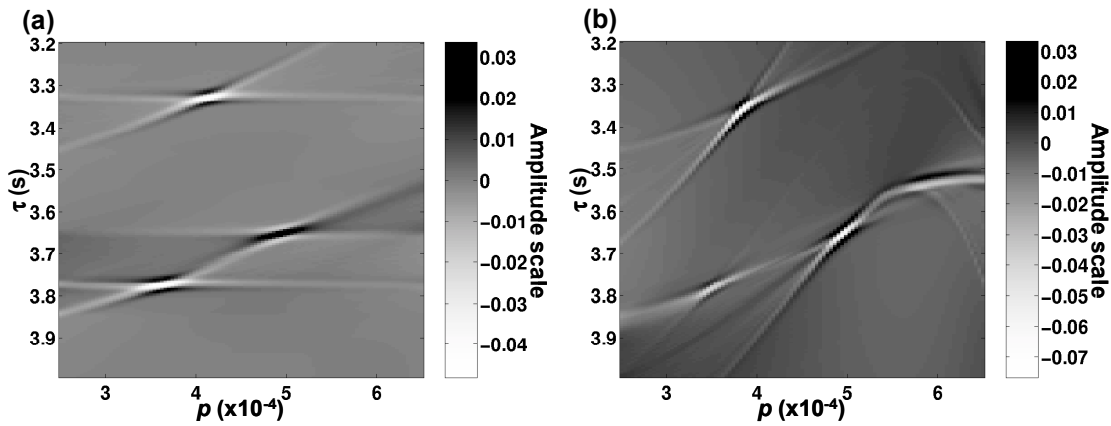


FIG. 4. Fourth-order hyperbolic Radon transform applied to (a) 0- to 2750-m offset (precritical for converted-wave) and (b) 2750- to 5000-m offset (converted-wave postcritical offsets).

increase in diagonal smearing from far offsets may be corrected by applying a taper on the far offsets only. The method of weighting allowed for discrimination of each type of energy analyzed and might prove advantageous for designing substantially more accurate mutes for the removal of unwanted energy.

The nonhyperbolic nature of mode-converted energy typically allows for far-offset amplitudes to be diminished by stacking alone. The removal of near-offset converted-wave events plus stacking may be a sufficient technique for diminishing converted-wave energy. In this case, applying the Radon transform only to near offsets with lower p -values would reduce computation time and expense of the algorithm. Alternatively, employing the multiple-hyperbolic transform may allow for a similar type of energy-partitioning removal. Results revealed efficient separation of near- and far-offset focused events in the multiple-hyperbolic Radon domain, although smearing due to limited-aperture data was prominent. The disadvantage of this method is that it is tuned for a certain focusing depth, and may be expensive for effective application to entire data sets.

The t^2 -stretched parabolic transform produced well focused events in the Radon domain and may be the least expensive algorithm to apply to data. However, stretching and unstretching may degrade the data by introducing further aliasing effects, and this must be considered when applying the method to real data. Although the fourth-order NMO equation also relies on a stretched data input, results obtained after application showed enhanced focusing of events, and aliasing does not appear to be a damaging factor for the model. The fourth-order equation requires extra parameters that must be adjusted for a specific event, thus increasing the expense of the algorithm. Introducing a ‘fudge’ factor relating μ_2 (slowness²) to μ_4 and t_0 may provide an alternative to tuning in this method.

Further testing of the effects of these algorithms on different models is necessary to prove the results implied by these tests. In addition to what has been presented in this work, all of the transforms can be applied before and after NMO or prestack depth migration for better removal of coherent energy and more accurate velocity analysis.

CONCLUSIONS

Weighting of the data can provide a method of discrimination of coherent noise from primary events. The t^2 -stretched parabolic transform produced accurate focusing of all events and might be the most robust algorithm available for separation of coherent events. Variations of the fourth-order nonhyperbolic and multiple-hyperbolic transforms may have increased focusing power for events but currently involve extra parameters that must be tuned for specific reflections. Future efforts involving modifications of these transforms have the potential to make them more robust to use on entire data sets.

FUTURE WORK

Assuming that the AVO responses of reflections are unknown makes the problem of precise focusing in the Radon domain too ill posed to allow application of a weighting to account for these effects in a robust way. As an alternative, a weighting function applied within the Radon operator may have better success. This method will be investigated to create an iterative process of tuning constants A and B of the function $A + Bx^2$ in the linear operator.

Castle (1994) described various traveltimes equations and concluded the shifted-hyperbola equation is the most practical NMO equation. He showed that for long offsets (offset > depth) the shifted hyperbola resembles the actual ray-traced response better than the standard Dix equation. We are currently exploring implementation of a shifted-hyperbolic transform with ‘fudge’ factors to avoid the need to tune for specific events. We are also testing application of these transforms in the high-resolution Radon algorithm.

ACKNOWLEDGEMENTS

We would like to thank the CREWES sponsors for their support of this research. We would also like to thank Dr. Mauricio Sacchi and Marco Perez for useful discussions and suggestions.

REFERENCES

- Carlson, D.H., 1997, 3D long offset non-hyperbolic velocity analysis: 67th Ann. Internat. Mtg., Soc. Expl. Geophys., Expanded Abstracts, 1693-1694.
- Castle, R.J., 1994, A theory of normal moveout: *Geophysics*, **59**, 983-999.
- Foster, D.J. and Mosher, C.C., 1992, Suppression of multiple reflections using the Radon transform: *Geophysics*, **57**, 386-395.
- Kabir, M.M.N. and Marfurt, K.J., 1999, Toward true amplitude multiple removal: *The Leading Edge*, **18**, 66-73.
- Sacchi, M.D. and Ulrych, T.H., 1995, High-resolution velocity gathers and offset space reconstruction: *Geophysics*, **60**, 1169-1177.
- Taner, M.T. and Koehler, F., 1969, Velocity spectra—digital computer derivation and applications of velocity functions: *Geophysics*, **34**, 859-881.
- Thorson, J.R. and Claerbout, J.F., 1985, Velocity-stack and slant-stack stochastic inversion: *Geophysics*, **50**, 2727-2741.
- Yilmaz, O., 1989, Velocity-stack processing: *Geophys. Prosp.*, **37**, 357-382.